Applications of Statistics and Probability in Civil Engineering – Faber, Köhler & Nishijima (eds)

Comparative risk assessment of secondary structures in wide-span timber structures

S. Miraglia
Università degli Studi di Napoli "Federico II", Naples, Italy
Engineering Risk Analysis Group, TU München, Germany

P. Dietsch
Chair for Timber Structures and Building Construction, TU München, Germany

D. Straub
Engineering Risk Analysis Group, TU München, Germany

ABSTRACT: Secondary structures in wide-span timber roofs are either realized as statically determinate or indeterminate systems. The latter are often preferred since they are more efficient in utilizing the material and enable load distribution in case of a local damage, but they also facilitate progressive collapse. The aim of this study is to compare the performance of different configurations of secondary structures in wide-span timber roofs, with respect to reliability, robustness and risk. To this end, a risk assessment of three configurations is performed by considering (probabilistically) all possible failure scenarios of purlin elements in the roof. In this initial study, failure of the primary beams is not considered. The results show that the static determinate configuration leads to a system that is less sensitive to local damages but has an overall higher risk. It must be further investigated whether this duality is also observed for the full system.

1 INTRODUCTION

During the past ten years, several collapses of wide span roofs occurred in Northern Europe during winter under high snow loads, in some cases leading to fatalities (Frühwald et al. 2007). Many of these roofs were built with timber elements (solid or glulam timber). These failures can be attributed to design errors, lack of quality of the elements or bad execution. In addition, failure can be caused by lack of maintenance or by unforeseen events that lead to a lower capacity (damage) or higher loads than expected. The failures most likely originate from errors made during the design phase, followed by errors made during the execution, while failures due to material deficiencies or maintenance were relatively uncommon, which was also found in an extensive study by Ellingwood (1987) that compiled results from a series of investigations on failed structures during the years 1979–1985.

In this context, attempts have been made to evaluate the robustness of wide span timber roofs (e.g. Kirkegaard and Sørensen 2008, Cizmar et al. 2009, and Dietsch & Winter 2010). These studies were performed within the framework of the COST action on robustness of structures. Generally, robustness of a structure is understood as the insensitivity to local failure and the avoidance of progressive collapse. It is a property of the structure itself, independent of possible causes of initial local failure (Starossek 2006). Many authors (Starossek et al 2008, Ionite et al. 2009) relate robustness to structural redundancy, which requires static indeterminacy and the avoidance of progressive collapse. Baker et al. (2008) use the ratio between direct and indirect expected damage as a measure of robustness. This definition also includes the consequences of failure, and it requires computation of the risk (direct and indirect).

Against this background, the goal of this study is to investigate the behavior of a wide span timber roof with a secondary structure designed according to three different structural configurations (simply-supported, continuous and lap-jointed purlins). These configurations were subject to a previous deterministic analysis of the system of primary elements (beams) and secondary elements (purlins) carried out by Dietsch & Winter (2010). In the present study, a risk assessment of the three systems is performed by considering (probabilistically) all possible failure scenarios. An intermediate result of the risk assessment is the probability

distribution of the consequences given a failure of the system; this distribution can be interpreted as a measure of robustness. The assessment also accounts for the possibility of systematic errors (which are modeled by weakened sections that occur randomly in the secondary structure).

2 CASE STUDY

The structural system studied is exemplary for common structural designs for wide-span roofs of sport-arenas, industrial factories or farm storage buildings, see Figure 1. The investigated roof covers an area of $\ell \times w = 30.0 \times 20.0$ m^2 and is supported by 6 primary pitched cambered beams at a distance of 6.0 m. In this study, these primary beams will be assumed intact (i.e. their probability of failure is zero).

The secondary elements (purlins) are mounted on the primary elements, which feature a pitch angle of 10°. This system has been subject to a previous deterministic analysis (Dietsch and Winter 2010), where four different configurations of purlins were considered: (a) simply supported purlins; (b) continuous purlins; (c) purlins in a Gerber system and (d) lap-jointed purlins. For the present study, three different configurations were chosen as depicted in Figure 2: (a) purlins designed as simply supported elements; (b) purlins designed as continuous beams; (c) purlins designed as lap-jointed beams.

The purlins are made from solid structural timber, which is commonly applied for secondary structures in wide-span timber roofs due to its guaranteed properties resulting from a controlled manufacturing process. The timber strength class

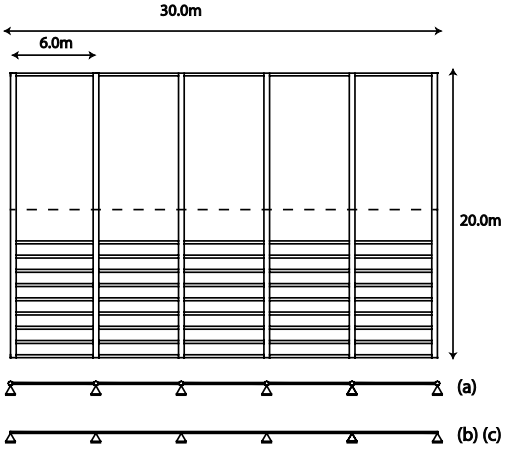

Figure 1. Geometry of the roof (Dietsch and Winter 2010).

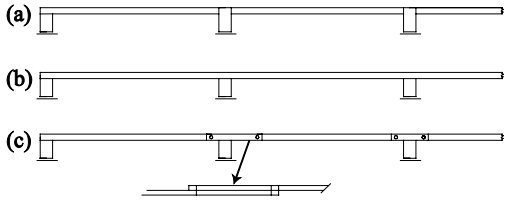

Figure 2. Three investigated purlin configurations.

used is C24 featuring a characteristic value of the bending strength $f_{m,k} = 24$ N/mm^2 according to EN 338 (2003). The purlins feature a cross section of $b \times h = 100 \times 200$ mm^2. The distance between the axis of the purlins is chosen so that the utilization factor according to EC5 (2004) is in the range $0.9 < \eta < 1$. The resulting distances e_p between purlins are: a) 1.0 m, b) 1.2 m and c) 1.6 m.

3 RISK ASSESSMENT

In the following, the risk associated with structural failure of the secondary system shall be computed. The consequences of these failures are considered to be proportional to the failed area of the roof A_F. Since there is no interest in computing absolute values of the risk, the risk can be defined as:

$$Risk = \mathrm{E}[A_F] = \int_0^{A_{roof}} a\, f_{A_F}(a)da \tag{1}$$

where E[ ] denotes the expectation operation and $f_{A_F}(a)$ is the probability density function (PDF) of the failed area.

In the analysis, we account for the possibility of a systematic weakening of the structure, which can be due to errors in the production and/or construction process. Let D be the event that such errors are present. Two separate material models are employed to compute $f_{A_F|\bar{D}}(a)$ and $f_{A_F|D}(a)$, as described in 3.3. The unconditioned PDF of the failed area is then

$$f_{A_F}(a) = f_{A_F|\bar{D}}(a)Pr(\bar{D}) + f_{A_F|D}(a)Pr(D) \tag{2}$$

where Pr(D) is the probability that a systematic weakening of the structure is present.

Regular design procedures are based on the assumption that systematic errors are prevented by quality control and other measures, i.e. it is assumed that $Pr(D) = 0$. Since robustness can be interpreted as the ability of the structure to sustain unforeseen actions, an indicator for robustness is the difference between the total risk, calculated

with Eqs.(1) and (2) and $Pr(D) > 0$, and the risk conditional on no errors, calculated with Eqs. (1) and (2) and $Pr(D) = 0$.

3.1 *Structural model*

For this analysis, only the bending failure mode is considered, shear failures, buckling failures and failures of joints are neglected, since in this case the bending failure is the main failure mechanism. Bending failure at cross-section j is described by the limit state function:

$$g_j = 1 - \left(\frac{M_{sx,j}}{M_{Rx,j}} + \frac{M_{Sy,j}}{M_{Ry,j}} \right) \tag{3}$$

$M_{Si,j}$ denotes the bending moment and $M_{Ri,j}$ denotes the bending capacity at cross section j in direction i. (We have a two-axial stress field due to the roof inclination of 10°) This limit state function is obtained by a first-order approximation of the limit of the resistance domain in the elastic stress-deformation field given in the EC5. Several authors (e.g. Cizmar et al. 2009, Kirkegaard et al 2008, Köhler 2007, Toratti et al. 2007) introduce a correction factor in the limit state function to account for the approximation made by this failure criterion. Since we believe that further investigation is necessary to better understand this factor, it is omitted in this study.

The bending moments are given as

$$M_{Sx,j} = a_{lx,j}(\mathrm{Q} \cdot C + G \cdot a_{cs} + P) \tag{4}$$

$$M_{Sy,j} = a_{ly,j}(\mathrm{Q} \cdot C + G \cdot a_{cs} + P) \tag{5}$$

where $a_{lx,j}$, $a_{ly,j}$ are load coefficients that depend on the structural configuration (a-c) and the location j along the longitudinal axis; a_{cs} is the cross section area of the purlins; the remaining variables are random variables describing the loads:

- Snow load on the ground Q;
- Shape factor C (snow load on the roof);
- Timber specific weight G;
- Permanent load P.

The bending capacities in Eq. (3) are described by

$$M_{Rx,j} = R_j \cdot \frac{2I_x}{d_y} \tag{6}$$

$$M_{Ry,j} = R_j \cdot \frac{2I_y}{d_x} \tag{7}$$

where R_j is the bending strength at cross section j, I_x and I_y are the inertia of the section and d_x, d_y are the width and depth of the purlins. The resistance of the elements is computed neglecting any time-dependency of the property of the material.

Each purlin is evaluated at discrete cross sections at distances of 0.5 m along its longitudinal axis, based on the approximate distance between weak sections (e.g. knots) in the timber (Thelandersson et al. 2003). Failure at a section j occurs when $g_j \leq 0$, where g_j is defined by Eq. (3). The purlin is modeled as a series system, so any failure of a section leads to failure of the purlin. Failure of a purlin leads to changes in the static scheme for configurations (b) and (c). Therefore, upon failure of one or more sections, the coefficients $a_{lx,j}$ and $a_{ly,j}$ in Eqs. (4) and (5) are recalculated and all sections are then evaluated with these values. In this way, the possibility of progressive failures is accounted for. This is illustrated in Figure 3.

Furthermore, failure of the roof system F is defined as the failure of one or more purlins. Therefore, the roof fails, when any of the discrete elements fail. This is justified by considering that the failure of an element will be detected immediately and corrective actions will be taken upon failure of one element.

3.2 *Probabilistic model*

The probabilistic model of the loads and of timber material properties is based on the Probabilistic Model Code of the Joint Committee of Structural Safety (JCSS 2006).

The specific weight G for structural timber is modeled by a Normal distribution with mean 4.2 kN/m^3 and a coefficient of variation (COV) of 10%. Geometrical properties of the purlins are assumed to be deterministic due to the quality control of the manufacturing process. The permanent load (from the roofing) is assumed to be Normal

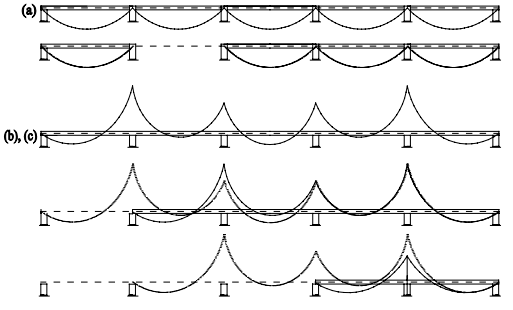

Figure 3. A possible failure scenario for the three configurations.

distributed with mean value of 0.4 kN/m² and COV = 0.1 (Dietsch and Winter 2010, JCSS 2006).

The snow load Q varies with time. Because we are neglecting duration of load effects, it is sufficient to model the maximum snow loads during a snow event. We assume that snow events occur according to a Poisson process with rate $\lambda = 1.175$ per year; the maximum snow load in each event Q_m is then modeled by a Gumbel distribution with mean 0.384 kN/m² and COV = 0.4. With this model, the characteristic value of the annual maximum snow load equals 0.8 kN/m², which corresponds to snow zone 1 in Germany at an altitude of about 480 m above sea level, see DIN EN 1991-1-3/NA (2010).

Figure 4 shows one realization of the snow load process, where t_i are the times of occurrence of the snow events and Q_{mi} are the snow loads at the events.

With the model of snow load given above, it is necessary to compute the distribution of the annual maximum snow load Q_{max}, as described in the following.

Let n be the number of snow events in a year and let Q_n be the maximum snow load in the n snow events. The cumulative probability function (CDF) of Q_n is obtained as a function of the CDF of the maximum snow load in each event Q_m as

$$F_{Qn}(q) = [F_{Qm}(q)]^n \tag{8}$$

The number of snow events per year is a random variable with probability mass function (PMF) $p_N(n)$. The CDF of the annual maximum snow load is therefore

$$F_{Qmax}(q) = \sum_{i=0}^{\infty} \left[F_{Q_m}(q) \right]^n \cdot p_N(n) \tag{9}$$

$p_N(n)$ is the Poisson PMF with parameter $\lambda T = 1.175$ and $F_{Qm}(q)$ is the Gumbel CDF with parameters a and b. Inserting in Eq.(8), the unconditioned CDF of the annual maximum snow load is:

$$\begin{aligned} F_{Q\max}(q) &= \sum_{n=0}^{\infty} \left\{ \exp\left[-\exp\left(-\frac{q-b}{a} \right) \right] \right\}^n \frac{(\lambda T)^n}{n!} \exp(-\lambda T) \\ &= \exp\left\{ \lambda T \left[\exp\left[-\exp\left(-\frac{q-b}{a} \right) \right] - 1s \right] \right\} \end{aligned} \tag{10}$$

The load on the ground, $Q(t)$, is transformed to the snow load on the roof by multiplying it with the shape factor C. The shape factor is model by a Gumbel distribution with mean $\mu_C = 0.78$ and COV equal to 0.35, following Sanpaolesi (1999) for a 10° pitch. This value accounts for the redistribution of the snow due to wind.

Uncertainty in the bending strength R is caused mainly by non-homogeneous material characteristics. Timber contains growth defects in the form of knots (Figure 5), fissures, zones of compressed wood, bark pockets, wane and resin pockets and changing fiber orientation, all of which lead to an increased variability of material strength.

Solid timber, like other types of structural timber, displays considerable strength variability between and within structural members, which must be accounted for in reliability analysis. To this end, it is commonly assumed that the strength along the beam (clear wood) is constant except within the section in which a defect occurs (weak zone) (Thelandersson et al. 2003, Piazza et al. 2005, Köhler 2007). The clear wood strength and the weak zone strength are described by stochastic variables, while the occurrences of the weak zones can be modeled as a Poisson process (JCSS 2006) or Gamma distributed (Köhler 2007). Here, we model the variability of timber strength according to the Isaksson Model (as reported in Thelandersson et al. 2003), summarized in the following.

It is assumed that the bending resistance within one section j of 0.5 m length is constant and is defined by

$$R_{ij} = \exp(\mu_{\ln R} + \varpi_i + \chi_{ij}) \tag{11}$$

where the index i indicates the purlin. Here, $\mu_{\ln R}$ is the logarithmic mean of the bending strength, ϖ_i is

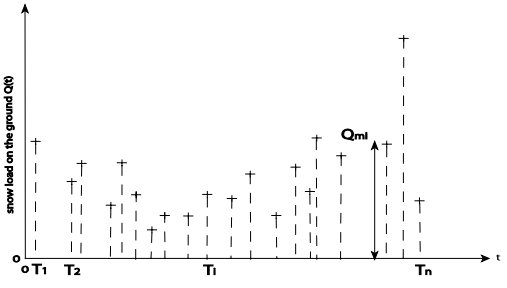

Figure 4. Train pulse of the snow load on the ground.

Figure 5. Presence of defects (knots) in a timber element.

a factor that accounts for the purlin-to-purlin variability and χ_{ij} is a factor that accounts for the variability among cross sections *j*. Figure 6 illustrates the model.

The factor ϖ_i is Normal distributed with zero mean and standard deviation $\sigma_{\varpi} = \sqrt{0.4\sigma^2_{\ln R}}$, where $\sigma_{\ln R}$ is the standard deviation of $\ln R_{ij}$. The factor χ_{ij} is also Normal distributed with zero mean and standard deviation $\sigma_{\chi} = \sqrt{0.6\sigma^2_{\ln R}}$. It is assumed that ϖ_i and χ_{ij} are statistically independent.

From this model, it follows that the logarithm of bending strengths $\ln R_{ij}$ of the cross sections $j = 1, \ldots, n_j$ in a single purlin i are correlated Normal random variables with correlation coefficients:

$$\rho_{\ln R} = \frac{\sigma^2_{\varpi}}{\sigma^2_{\varpi} + \sigma^2_{\chi}} = 0.4 \qquad (12)$$

In the case of a timber beam of class C24, we compute the parameters of the strength model from the characteristic value of bending strength (24 *MPa*) and imposing a COV = 0.25 (JCSS 2006). The resulting parameter of the Lognormal distribution are $\mu_{\ln R}$ =3.58 and $\sigma_{\ln R}$.

The probabilistic model is summarized in Table 1.

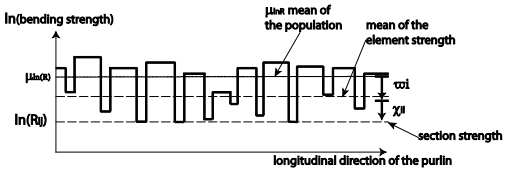

Figure 6. Lengthwise variation of bending strength for Isaksson model (JCSS 2006).

Table 1. Stochastic model of timber elements.

	r.v.	Distribution	μ	COV
Snow load on the ground [kN/m²]	Q	Gumbel	0.384	0.40
Occurrence [1/y]	T	Poisson	1.175	0.92
Shape Factor [\]	C	Gumbel	0.78	0.35
Density [kN/m³]	G	Normal	4.20	0.10
Permanent load [kN/m²]	P	Normal	0.4	0.10
Bending strength [MPa]	R_{ij}	Lognormal	36.97	0.25
Bending strength [MPa]	R_{Dij}	Lognormal	29.57	0.25

3.3 *Modeling systematic errors in the structure*

In order to study the behavior of different structural configurations when systematic errors are present, we need to define a probabilistic model for these errors. Following Eq.(2), the event that systematic errors are present is denoted by D. Due to their nature, no probabilistic models of such errors exist; therefore, our model will be purely hypothetical and serves only to compare the different structural configurations.

We assume that systematic errors D can occur as design errors, manufacture error (wrong cross section, wrong strength grade) or execution errors (production, execution of holes in the joints, finger joints etc.), leading to significant reductions in bending strength locally, e.g. at the finger joints. We model the occurrence of these weak sections by a Bernoulli process with rate $p = 0.30$. The strength at the weak sections, R_D, is modeled by a Lognormal distribution whose mean value is reduced by 20% compared to the intact sections. The COV of R_D is identical to the one of the intact element.

4 NUMERICAL INVESTIGATION

4.1 *Computations*

Computations are performed with Monte Carlo Simulations (MCS) with 10^5 samples. MCS enable the evaluation of the full distribution of the damaged area, $f_{A_F|\bar{D}}(a)$ and $f_{A_F|D}(a)$, as required in Eq. (2). As an independent check, and to assess the sensitivity of the results on the probabilistic model, we additionally use First-Order Reliability Method (FORM) to compute the probability of system failure, $Pr(F(t))$.

4.2 *Results*

Table 2 summarizes the probability of failure of the critical sections for the three structural configurations, which correspond to the sections that are checked in the deterministic design. These calculations assume that there are no systematic errors in the purlins. The results confirm that the design reliability is identical for the three configurations, which is expected since all three were designed to have the same utilization factor. It is furthermore noted that the reliability index is lower than the target value given in Eurocode 0, which is $\beta = 4.7$ for a one-year reference period. The FORM sensitivity factors presented in Table 3 show that the uncertainty in the snow load Q, the shape factor C and the bending strength R determine the reliability. The difference between the calculated reliability indexes and the target value of Eurocode 0 might

Table 2. Probability of failure of a critical section j, $Pr(F_j(1yr)\,|\,\bar{D})$ and corresponding reliability index β_j.

	$Pr(F_j(1yr)\,|\,\bar{D})$	β_j
(a) Simply supp.	$7.4{\cdot}10^{-6}$	4.33
(b) Continuous	$7.9{\cdot}10^{-6}$	4.32
(c) Lap-Jointed	$7.0{\cdot}10^{-6}$	4.34

Table 3. FORM sensitivity factors for a single purlin.

	α_Q	α_c	α_G	α_p	α_R
(a) Simply supp.	0.604	0.597	0.0080	0.037	–0.526
(b) Continuous	0.604	0.597	0.0078	0.037	–0.526
(c) Lap-Jointed	0.604	0.597	0.0077	0.037	–0.526

be explained by the significant uncertainty in the shape factor C.

Table 4 summarizes the probability of system failure in 50 years given that there are no systematic errors $Pr(F\,|\,\bar{D})$ for the three structural configurations. As observed, the reliability of the three systems is not identical, due to the varying numbers of critical sections. Configuration (a) has the largest number, since it contains more purlins and each purlin has a critical section (in the middle of the spans). Configurations (b) and (c) have only two critical sections in each line (in the outer spans). Furthermore, configuration (c) has less purlins than (b) due to the larger possible distance between the purlins. The differences between the FORM and the MCS results in Table 4 can be explained by the approximations made in the FORM analysis.

Because degradation of the material has not been considered, the failure rate is approximately constant over the service life period.

Figure 7 shows the computed CDF of the failed area A_F conditional on the system having failed F and on the absence of systematic errors $\bar{D}, F_{A_F|F,\bar{D}}(a)$. It can be observed that a failure in the structural system with simply supported purlins (a) results in smaller damages than the other configurations. In configuration (a), a smaller number of purlins (and consequently a smaller proportion of the roof area) will fail. In the other two, statically indeterminate, configurations, progressive collapse mechanisms lead to a larger number of purlin failures once the first section has failed (see Figure 3). The continuous purlin configuration (b) behaves better than the lap-jointed configuration (c). Table 5 lists the probability of system failure given that there is a systematic weakening of the system, $Pr(F|D)$, for the three structural configurations.

Table 4. Probability of system failure $Pr(F(50yr)\,|\,\bar{D})$.

	MCS (95% confidence interval)	FORM
(a) Simply supp.	$4.51{\cdot}10{-}2 \div 4.76{\cdot}10{-}2$	$1.81{\cdot}10{-}2$
(b) Continuous	$1.75{\cdot}10{-}2 \div 1.92{\cdot}10{-}2$	$1.45{\cdot}10{-}2$
(c) Lap-Jointed	$1.39{\cdot}10{-}2 \div 1.54{\cdot}10{-}2$	$1.32{\cdot}10{-}2$

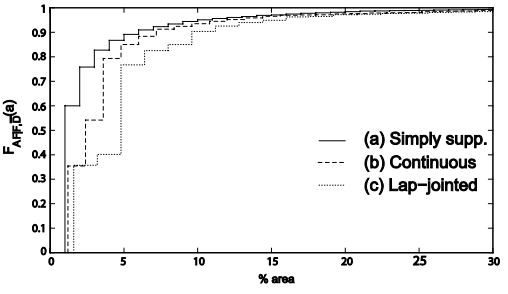

Figure 7. $F(A_F\,|\,F,\bar{D})$ for the three systems without systematic weakening.

As expected, this leads to an increase in the probability of system failure compared to the case of no weakening.

Figure 8 shows the computed CDF of the failed area A_F conditional on the system having failed F and on the presence of systematic weakening $F_{A_F|F,D}(a)$. The three configurations show the same trend as in the case of the error-free system (Figure 7), however, in the case of systematic weakening the average size of the failed area is slightly lower. This is explained by the fact that, in this case, the uncertainty in the capacity has a stronger effect. This leads to a decrease in the statistical dependence among failures of individual sections and, therefore, large numbers of purlin failures become less likely.

Table 6 lists the expected values of the size of the failed area A_F given system failure in both cases: the higher the static indeterminacy, the higher the expected area failed.

Following Eq. (2), we can compute $F_{A_F|F}$ (i.e. the distribution of the failed area when it is unknown whether a systematic weakening of the system is present or not) as

$$F_{A_F|F,D}(a) = F_{A_F|\bar{D}}(a)\,Pr(\bar{D}\,|\,F) + F_{A_F|D}(a)\,Pr(D\,|\,F) \qquad (13)$$

Table 5. Probability of system failure $Pr(F(50yr)|\bar{D})$.

confidence interval at 95%	$Pr(F(50yr)\|\bar{D})$ $p = 30\%$
(a) Simply supp.	$9.38\cdot10^{-2} \div 9.57\cdot10^{-2}$
(b) Continuous	$5.21\cdot10^{-2} \div 5.50\cdot10^{-2}$
(c) Lap-Jointed	$2.94\cdot10^{-2} \div 3.15\cdot10^{-2}$

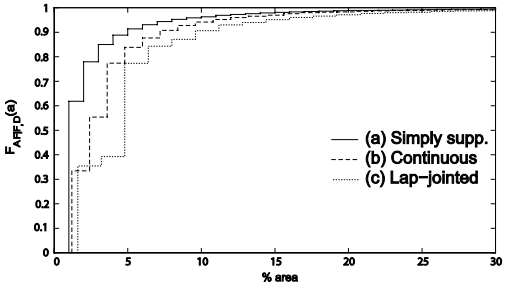

Figure 8. $F(A_F|F,D)$ for the three systems with systematic weakening.

Table 6. Expected value of area failed.

	$E[A_F \mid F,\bar{D}]$ $p = 0$	$E[A_F \mid F,D]$ $p = 30\%$
(a) Simply supp.	2.87	2.52
(b) Continuous	4.04	3.89
(c) Lap-Jointed	5.39	5.30

where the probability Pr(D|F) is computed by Bayes' rule as

$$Pr(D|F) = Pr(F|D)Pr(D)\,/Pr(F) \tag{14}$$

$$Pr(F) = Pr(F \mid D)Pr(D) + Pr(F \mid \bar{D})Pr(\bar{D}) \tag{15}$$

Figure 9 and Figure 10 show the CDF of the failed area A_F conditional on the system having failed F. In Figure 9 we assume a lower probability of having systematic errors ($Pr(D) = 0.01$) than in Figure 10 ($Pr(D) = 0.10$). However, it can be observed that the difference between the results obtained with these two assumptions is minor (as is the difference to the results obtained for the system without weakness). The reason is that the effect of the weakness on the conditional distribution is low, as seen from comparing Figure 7 with Figure 8.

Table 7 lists the expected values of the size of the failed area A_F given system failure F, for the two values of $Pr(D)$.

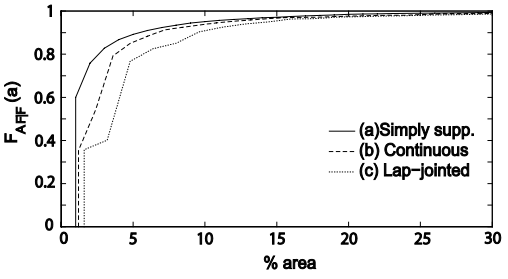

Figure 9. $F(A_F|F)$ for the three configurations for $Pr(D) = 1\%$.

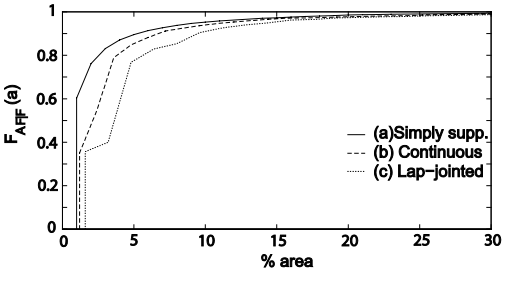

Figure 10. $F(A_F|F)$ for the three configurations for $Pr(D) = 10\%$.

Table 7. Expected value of area failed given the failure event (%).

	$E[A_F\|F]$ $Pr(D) = 1\%$	$E[A_F\|F]$ $Pr(D) = 10\%$
(a) Simply supp.	2.86	2.81
(b) Continuous	4.04	4.00
(c) Lap-Jointed	5.39	5.37

Table 8. Probability of the failed area exceeding 15% of the total area upon failure (for $Pr(D) = 0.1$).

	$1 - F(A_F = 15\%\|F)$
(a) Simply supp.	0.027
(b) Continuous	0.035
(c) Lap-Jointed	0.032

Table 9. Expected value of area failed (%).

	$E[A_F]$ $Pr(D) = 1\%$	$E[A_F]$ $Pr(D) = 10\%$
(a) Simply supp.	$1.3\cdot10^{-3}$	$1.4\cdot10^{-3}$
(b) Continuous	$0.8\cdot10^{-3}$	$0.9\cdot10^{-3}$
(c) Lap-Jointed	$0.8\cdot10^{-3}$	$0.9\cdot10^{-3}$

EN 1991-1-7 includes a requirement that a failure should not lead to a failed area in excess of 15% of the total area. To check this "robustness" criterion, we calculate the probability that the failed area exceeds 15% of the total area given a failure, Table 8.

Finally, the risk, which is defined as the expected size of the failed area $E[A_F]$ in Eq. (1), is summarized in Table 9.

5 DISCUSSION

When designing a structural system it must be ensured that none of the limit state conditions is violated, in accordance with the code. This ensures an acceptable reliability of the system. In addition, the system should be designed for robustness, for which, however, there are at present no commonly applied quantitative criteria. Finally, from a decision-theoretic point-of-view, the optimal structural design is the one minimizing the total expected cost (design and maintenance cost plus risk). In this study, we investigated different configurations of secondary structures in wide-span timber structures. All three configurations comply with the code requirements and the critical sections all have the same reliability (Table 2). However, the system reliability of the three configurations is different because of the varying number of elements and the fact that system failure is defined through a series system (Table 4).

In terms of robustness, it can be argued that structural system configuration (a) consisting of simply supported purlins is the optimal one, because a failure in this configuration leads to the smallest failed area (Figure 9 and Figure 10) and it has the lowest probability of not fulfilling the 15%-area requirement (Table 8). These calculations include the possibility of a random but systematic reduction of strength (e.g. due to gross errors).

However, the risk calculated for configuration (a) is higher than for configurations (b) and (c), which are statically indeterminate (Table 9). This is due to the fact that the probability of system failure is higher for configuration (a), even though the consequences are lower. Therefore, it is argued that despite the fact that configuration (a) is more robust, this study indicates that configurations (b) and (c) are more optimal. In addition, configuration (c) is the cheapest, thus supporting this choice of this configuration from a risk (or rather expected cost) perspective. This points to a general problem in the definition of robustness, which is beyond the scope of this paper, namely that a more robust system might often be less optimal from a risk analysis point-of-view. These conclusions, drawn from the results presented, are also dependent on the fact that the distances e_p between the purlins were adapted in order to receive the same utilization factor for all systems. In reality, the distances are based on requirements from the roof cladding. If the same distances would be applied to all systems, assuming a consistent utilization factor, the three systems would show a more similar behavior. If configurations (b) and (c) would be modified to have the same distance between purlins than (a), they would become slightly more robust but would also have a higher probability of system failure and thus exhibit a higher risk.

The presented study is limited in scope and not sufficient to make final conclusions on which configuration is optimal for secondary structures in wide-span timber structures, because of the assumption that the primary beams are intact. In future work, the model will be extended to include such failures. However, the results obtained from this study do provide valuable insight in the observed behavior (namely that the statically indeterminate configurations are less robust but more optimal) might also hold for other systems. The risk-based approach presented in this paper facilitates such investigations.

6 CONCLUSIONS

Three different configurations of secondary structures in wide-span timber structures are compared with respect to their reliability, robustness and risk. Despite the fact that all three systems are designed to have the same reliability in the critical sections, the statically indeterminate configurations have a higher system reliability due to the smaller number of elements. On the other hand, the configuration with exclusively statically determinate elements exhibits lower consequences in the case of failure, which can be interpreted as a higher robustness. However, this configuration has the highest risk. It is concluded that robustness and risk can be contradictory criteria.

REFERENCES

Baker J.W., Schubert M., Faber M.H., (2008). On the Assessment of robustness. Structural Safety, 30, 253–267.

Cizmar D., Sørensen J.D., Kirkegaard P.H. (2009). Reliability and Robustness evaluation of timber structures, Short Term Scientific Mission, COST E55 Action, DCE Technical Report, 58.

Dietsch P., Winter S. (2010). Robustness of Secondary Structures in wide-span Timber Structures. Proceedings WCTE 2010, Riva del Garda, Italy.

DIN EN 1991–1-3/NA (2010). National Annex – National determined Parameters – Eurocode 1: Actions on

Structures – Part 1–3: General Actions – Snow Loads. DIN Deutsches Institut für Normung e.V., Berlin.

Ellingwood B. (1987). Design and Construction error Effects on Structural Reliability. Journal of Structural Engineering, 113(2): 409–422.

EN 1995–1-1. (2004). Eurocode 5: Design of Timber Structures: Part1–1 General- Common rules and rules for buildings, European Committee for Standardization (CEN), Brussels.

EN 338 (2009). Structural timber - Strength classes, European Committee for Standardization (CEN), Brussels.

Frühwald E., Serrano E., Toratti T., Emilsson A., Thelandersson S. (2007). Design of safe timber structures-how can we learn from structural failures in concrete, steel and timber? Report TVBK-3053, Div. of Struct. Eng., Lund University, Sweden.

Ionite O.M., Tarann N., Budescu M., Banu C., Rominu S., Banala R. (2009). Robustness of civil Engineering Structures, a modern approach in structural design, Technical Report, Intersection, 6(4).

JCSS-Joint Committee on Structural Safety. (2008). Probabilistic Model Code, 12th draft, internet version: http://www.jcss.ethz.ch, 2000.

Kirkegaard P.H.-Sørensen J.D. (2008). A probabilistic Approach for Robustness Evaluation of Timber Structures, Technical report, 55, Aalborg University, Denmark.

Koehler J. (2007). Reliability of Timber Structures. IBK Bericht 301, ETH Zurich, Switzerland.

Piazza M., Tomasi R., Modena R. (2005). Strutture in legno, Materiale, calcolo e progetto secondo le nuove normative europee, Hoepli, Milan, Italy.

Sanpaolesi L. (1999). Scientific Support Activity in the field of Structural Stability of Civil Engineering works on Snow Loads- Final Report. University of Pisa, Italy.

Starossek U. (2006). Progressive collapse of Structures. Proceedings of the Annual conference of the Structural Engineering Committee of the Korean Society of Civil Engineers, Seoul, Korea.

Starossek U., Haberland M., (2008). Measures of Structural Robustness- Requirements and Applications, ASCE SEI 2008 Structures Congress-Crossing Borders, Vancouver, Canada.

Thelandersson S., Larsen H.J. (2003). Timber Engineering, Wiley & Sons, England.

Toratti T., Schnabl S., Turk G. (2007). Reliability Analysis of a glulam beam, Structural Safety, 29, 279–293.